in tetrahydrofuran was added by cannula, and the mixture stirred 4 days. After quenching with 50 mL of H_2O, the mixture was extracted with 40 mL of pentane. The organic phase was washed with 3 × 70-mL portions of H_2O, dried ($MgSO_4$), and filtered through basic alumina. Evaporation gave 0.42 g of **2-*d*** as a waxy solid, which was sublimed (35 °C, 0.3 Torr, coldfinger cooled with dry ice) to give material, mp 32-33 °C. ^1H NMR ($CDCl_3$) δ 2.96 (br s, 4 H), 1.53 (m, ca. 3 H), 1.36 (br d, J = 8.0 Hz, 2 H), 1.04 (d, J = 8.0 Hz, 2 H), 0.83 (m, 4 H). ^{13}C NMR ($CDCl_3$) δ 151.44 (C), 50.19 (CH_2), 42.80 (CH), 25.24 (CH_2), 24.90 (CD, t, J = 19.5 Hz). Integration of the ^1H NMR spectrum indicated 82% D incorporation.

Acknowledgment. This work was supported by the Swiss National Science Foundation (F.G., G.G.), the National Institutes of Health (Grant CA-12115; L.A.P., L.W.), and the donors of the Petroleum Research Fund, administered by the American Chemical Society (S.F.N., M.F.T.).

^{13}C NMR and X-ray Structure Determination of 1-(Arylazo)-2-naphthols. Intramolecular Proton Transfer between Nitrogen and Oxygen Atoms in the Solid State

Alejandro C. Olivieri,* Roxy B. Wilson,* Iain C. Paul,* and David Y. Curtin*

Contribution from the Department of Chemistry, University of Illinois—Urbana/Champaign, Urbana, Illinois 61801. *Received December 12, 1988*

Abstract: The tautomeric reaction involving a single proton transfer in 1-(phenylazo)-2-naphthol and its 4′-methoxy, ethoxy, and *N,N*-dimethylamino derivatives has been investigated with variable-temperature solution and high-resolution solid-state ^{13}C NMR spectroscopy. Crystal structures of the parent unsubstituted compound and the 4′-*N,N*-dimethylamino derivative have been determined. All of these compounds undergo a fast proton exchange on the NMR time scale between the tautomeric azo and hydrazone forms in both solution and the crystalline phase. Equilibrium compositions in the solid materials are similar to those measured in solution. Crystals of 1-(phenylazo)-2-naphthol are monoclinic, a = 27.875 (7), b = 6.028 (2), c = 14.928 (5) Å, β = 103.57 (2)°, the space group is $C2/c$ with Z = 8, and the structure at 213 K was refined to an R factor of 0.0414 on 1082 observed reflections. Crystals of 1-([4′-(dimethylamino)phenyl]azo)-2-naphthol are monoclinic, a = 7.604 (1), b = 7.970 (3), c = 24.381 (7) Å, β = 99.33 (2)°, the space group is $P2_1/c$ with Z = 4, and the structure at 193 K was refined to an R factor of 0.0405 on 1522 observed reflections.

Hydrogen-bonded systems, both in solution and in the solid phase, have attracted considerable attention over the years.[1-3] Especially interesting are those structures where hydrogens are transferred in a tautomeric change.[4,5] In the solid state, such proton transfers take place in an environment where packing forces may appreciably affect the dynamics of the reaction as well as the tautomeric composition.[6-9] A knowledge of these processes is fundamental to an understanding of the structure and behavior of such solids and could also have technological implications, as proton exchanges in solids have potential utility as the basis of optical data storage devices.[10-12]

This tautomeric behavior in solution has been recognized in a number of azo dyes.[13,14] Intramolecular proton transfers between nitrogen and oxygen atoms have been studied by various techniques, including visible spectrophotometry[15] and NMR spectroscopy.[16-25] The latter method has provided a quantitative measure of the relative amounts of the azo and hydrazone forms present in the equilibrium. In $CDCl_3$ solution at room temperature, 1-(phenylazo)-2-naphthol (**1**) has been found to exist as a rapidly exchanging mixture of ca. 70% of the hydrazone form

(1) Hamilton, W. C.; Ibers, J. A. *Hydrogen Bonding in Solids*; W. A. Benjamin: New York, 1968.
(2) Joesten, M. D.; Schaad, L. J. *Hydrogen Bonding*; Marcel Decker: New York, 1974.
(3) Schuster, P.; Zundel, G.; Sandorfy, C., Eds. *The Hydrogen Bond. Recent Developments in Theory and Experiments*; North-Holland: Amsterdam, 1976.
(4) Hibbert, F. *Adv. Phys. Org. Chem.* **1986**, *22*, 113.
(5) Wehrle, B.; Limbach, H. H.; Zimmermann, H. *Ber. Bunsen-Ges. Phys. Chem.* **1987**, *91*, 941.
(6) (a) Shiau, W. I.; Duesler, E. N.; Paul, I. C.; Curtin, D. Y.; Blann, W. G.; Fyfe, C. A. *J. Am. Chem. Soc.* **1980**, *102*, 4546. (b) Herbstein, F. H.; Kapon, M.; Reisner, G. M.; Lehman, M. S.; Kress, R. B.; Wilson, R. B.; Shiau, W. I.; Duesler, E. N.; Paul, I. C.; Curtin, D. Y. *Proc. R. Soc. London* **1985**, *A399*, 295-319.
(7) Szeverenyi, N. M.; Bax, A.; Maciel, G. E. *J. Am. Chem. Soc.* **1983**, *105*, 2579.
(8) Limbach, H. H.; Henning, J.; Kendrick, R. D.; Yannoni, C. S. *J. Am. Chem. Soc.* **1984**, *106*, 4059.
(9) Frydman, L.; Olivieri, A. C.; Diaz, L. E.; Frydman, B.; Morin, F. G.; Mayne, C. L.; Grant, D. M.; Adler, A. D. *J. Am. Chem. Soc.* **1988**, *110*, 336.
(10) deVries, H.; Wiersma, D. A. *J. Chem. Phys.* **1980**, *72*, 1851.
(11) Rebane, L.; Gorokhovskii, A. A.; Kikas, J. V. *Appl. Phys. B* **1982**, *29*, 235.
(12) Romagnoli, M.; Moerner, W. E.; Schellenberg, F. M.; Levenson, M. D.; Bjorklund, G. C. *J. Opt. Soc. Am. B* **1984**, *341*, 1.
(13) Venkataraman, K. *Chemistry of Synthetic Dyes*; Academic Press: New York, 1952; Vol. 1.
(14) Zollinger, H. *Azo and Diazo Chemistry*; Wiley-Interscience: New York, 1961.
(15) Burawoy, A.; Salem, A. G.; Thompson, A. R. *J. Chem. Soc.* **1952**, 4793.
(16) Bekárek, V.; Rotschein, K.; Vetesnik, P.; Vecera, M. *Tetrahedron Lett.* **1968**, 3711.
(17) Berrie, A. H.; Hampson, P.; Longworth, S. W.; Mathias, A. *J. Chem. Soc. B* **1968**, 1308.
(18) Bekárek, V.; Dobáš, J.; Socha, J.; Vetešnik, P.; Vecera, M. *Coll. Czeck. Chem. Commun.* **1970**, *35*, 1406.
(19) Lycka, A.; Šnobl, D.; Machácek, V.; Vecera, M. *Org. Magn. Reson.* **1981**, *15*, 390.
(20) Lycka, A.; Šnobl, D.; Machácek, V.; Vecera, M. *Org. Magn. Reson.* **1981**, *16*, 17.
(21) Miyahara, M. *Eisei Shikensho Hokoku* **1982**, *100*, 135; *Chem. Abstr.* **1984**, *100*, 5716f.
(22) Lycka, A.; Hansen, P. E. *Org. Magn. Reson.* **1984**, *22*, 569.
(23) Federov, L. A.; Zhukov, M. S.; Korsakov, I. V.; Dedkov, Yu. M.; Ermakov, A. I. *Izv. Akad. Nauk. SSSR, Ser. Khim.* **1984**, 1763.
(24) Hansen, P.; Lycka, A. *Magn. Reson. Chem.* **1986**, *24*, 772.
(25) Gelbcke, M.; Masiala Tsodo, C. *Anal. Lett.* **1980**, *A13*, 975.

0002-7863/89/1511-5525$01.50/0

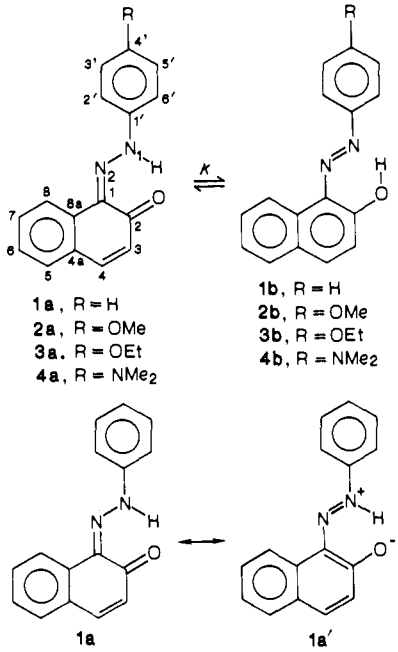

1a and 30% of the azo form **1b**.[16-19] Substituents attached to C(4') are known to affect the position of the equilibrium: electron-donating R groups tend to favor the azo form, whereas electron-withdrawing groups stabilize the hydrazone structure.[15,21] When R = NO_2 or SO_3Na, the equilibrium is mainly dominated by the hydrazone form,[15,24] while in the case R = OMe the equilibrium mixture is approximately equimolar.[15,21]

Early IR studies in the solid state of a series of 4'-substituted 1-(phenylazo)-2-naphthols revealed the presence of both keto and azo bands in some cases, although it was not possible to distinguish between a dynamic proton exchange and static disorder.[26] The reported X-ray diffraction analyses of several azo dyes favored the hydrazone form;[27-33] although the observed N(1)-N(2) and C(1)-N(2) bond lengths did not exactly match those expected for a single and a double bond, respectively, delocalization effects were invoked to explain these results. It should be noted that the X-ray studies were conducted on compounds bearing substituent groups in the phenyl ring which, in solution, were known preferentially to stabilize the hydrazone structure.

High-resolution solid-state NMR, combining cross-polarization (CP),[34] magic-angle spinning (MAS),[35] and high-power ^1H decoupling, has provided important dynamical and structural information on proton-exchanging solids.[6-9] A ^{13}C CPMAS NMR study of solid 1-((2'-nitro-4'-methylphenyl)azo)-, 1-((2'-nitro-4'-chlorophenyl)azo)-, and 1-((4'-nitrophenylazo))-2-naphthol (compounds **5**, **6**, and **7**, respectively) has been reported.[36] The results were in agreement with the diffraction data, confirming the existence of these compounds in the solid mainly as hydrazone structures. While the present paper was in preparation, an ^{15}N CP MAS study of ^{15}N doubly enriched **1** at variable temperatures was published, showing that this compound exists in the solid phase as a rapidly interconverting equilibrium mixture, with the tautomeric composition displaced more toward the hydrazone form than was found in solution.[37]

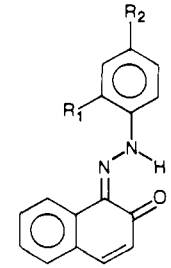

This paper reports a study of the proton-transfer reaction in **1-4** combining natural-abundance ^{13}C CP MAS NMR spectroscopy in the solid state and in solution with X-ray diffraction determination of the structures of **1** and **4**.

Experimental Section

All samples were synthesized according to known procedures.[38] Solid powders for the CP MAS studies were obtained by grinding material recrystallized from the same solvent used to obtain the X-ray-quality single crystals.

Solution ^{13}C NMR measurements were carried out in a General Electric GN300NB spectrometer operating at a frequency of 75.5 MHz. Variable-temperature spectra were collected in CD_2Cl_2 or $CDCl_3$ solution depending on the sample; the resonances were referenced against the solvent signal and then converted to the TMS scale. Typical spectral conditions were as follows: spectral width, 20 kHz; acquisition time, 819.2 ms; carbon pulse width, 25 μs; recycle delay, 2 s; 32K memory; number of acquisitions, 100-500 depending on temperature and solubility of samples. Temperatures were measured with a thermocouple on the cooling gas and are considered accurate within ±1 K.

Solid-state ^{13}C CP MAS NMR spectra at 50.2 MHz were recorded on a Chemagnetics A-200S spectrometer in the Department of Medicinal Chemistry and Pharmacognosy at Purdue University. Samples were packed in either Kel-F or zirconium rotors and spun at about 3 and 5.5 kHz, respectively. Spectral conditions were as follows: spectral width, 15 kHz; cross-polarization time, 4 ms; proton 90° pulse, 5.4 μs; recycle delay, 2 s; number of acquisitions, 3000-8000. Dipolar-dephased spectra were obtained by turning off the high-power ^1H decoupling 40 μs prior to acquisition.

^{13}C CP MAS NMR spectra (75.5 MHz) were also obtained on a General Electric GN300WB instrument. Kel-F rotors were filled with powder samples and spun at about 3 kHz. As this spinning rate was not enough to suppress side bands, the TOSS technique was employed.[39] Normal conditions for spectral recording were as follows: spectral width, 30 kHz; cross-polarization time, 5 ms; proton 90° pulse, 9.5 μs; recycle delay, 2 s; 4K memory; number of acquisitions, 1500-3000. Low-temperature measurements (down to 183 K) were made by cooling the driving gas in liquid N_2. Temperatures were determined by using a previously calibrated thermocouple and may be considered correct within ±1 K. Dipolar dephasing was achieved by applying no proton decoupling during one of the delays of the TOSS pulse sequence (ca. 60 μs).

X-ray data collection was carried out on a Syntex $P2_1$ automated four-circle diffractometer or on an Enraf-Nonius CAD-4 κ-axis instrument. Crystal data for **1** and **4** at two different temperatures as well as details of data collection are given in Table I. Structures were solved by using the SHELXS86 package of crystallographic programs[40] and refined by full-matrix least-squares techniques.[41] All hydrogens were located by difference Fourier techniques. Least-squares refinement was based on the reflections that had $I > 1.96\sigma(I)$ and included positional parameters for all atoms, anisotropic thermal parameters for non-hydrogen atoms, and isotropic thermal parameters for the hydrogen atoms. Different refinement models for the tautomeric hydrogen atom were attempted. In the case of **1** at 213 K, this hydrogen appeared on a dif-

(26) Morgan, K. J. *J. Chem. Soc.* **1961**, 2151.
(27) Kobelt, D.; Paulus, E. F.; Kunstmann, E. *Acta Crystallogr.* **1972**, *B28*, 1319.
(28) Kobelt, D.; Paulus, E. F.; Kunstmann, W. *Z. Kristallogr.* **1974**, *139*, 15.
(29) Whitaker, A. *Z. Kristallogr.* **1977**, *145*, 271.
(30) Whitaker, A. *Z. Kristallogr.* **1977**, *146*, 173.
(31) Whitaker, A. *Z. Kristallogr.* **1978**, *147*, 99.
(32) Whitaker, A. *Z. Kristallogr.* **1980**, *152*, 227.
(33) Grainger, C. T.; McConnell, J. F. *Acta Crystallogr.* **1979**, *B25*, 1962.
(34) Schaeffer, J.; Stejskal, E. O.; Buchdahl, R. *Macromolecules* **1975**, *8*, 291.
(35) Andrew, E. R. *Progr. Nucl. Magn. Reson. Spectrosc.* **1971**, *8*, 1.
(36) Harris, R. K.; Jonsen, P.; Packer, K. J.; Campbell, C. D. *Magn. Reson. Chem.* **1986**, *24*, 977.
(37) Lycka, A.; Jirman, J.; Schneider, B.; Straka, J. *Magn. Reson. Chem.* **1988**, *26*, 507.
(38) Liebermann, C. *Chem. Ber.* **1883**, *16*, 2858.
(39) Dixon, W. T. *J. Chem. Phys.* **1982**, *77*, 1800. Dixon, W. T.; Schaeffer, J.; Sefcik, M. D.; Stejskal, E. O.; McKay, R. A. *J. Magn. Reson.* **1982**, *49*, 341.
(40) Sheldrick, G. M. SHELX86. *Direct Methods Package for the Solution of Crystal Structures from Diffraction Data*; University of Cambridge, England, 1986.
(41) Sheldrick, G. M. SHELX76. *Program for Crystal Structure Determination*; University of Cambridge, England, 1976.

Table I. Crystal and Collection Data for Compounds **1** and **4**

	compound (temp, K)			
	1 (300)	**1** (213)	**4** (300)	**4** (193)
cryst syst	monoclinic	monoclinic	monoclinic	monoclinic
space group	$C2/c$	$C2/c$	$P2_1/c$	$P2_1/c$
formula	$C_{16}H_{12}N_2O$	$C_{16}H_{12}N_2O$	$C_{18}H_{17}N_3O$	$C_{18}H_{17}N_3O$
M	248.28	248.28	291.35	291.35
a, Å	28.164 (14)	27.875 (7)	7.624 (1)	7.604 (1)
b, Å	6.041 (2)	6.028 (2)	8.038 (2)	7.970 (3)
c, Å	15.209 (9)	14.928 (5)	24.709 (6)	24.381 (7)
β, deg	103.19 (4)	103.57 (2)	99.12 (1)	99.33 (2)
V, Å^3	2519 (2)	2434 (3)	1495 (8)	1458 (1)
d, g/cm	1.309	1.355	1.294	1.327
cryst form	prism	prism	tabular	tabular
dim, mm	0.1; 0.2; 0.8	0.1; 0.2; 0.5	0.2; 0.5; 0.6	0.2; 0.5; 0.6
solvent	acetone	acetone	chloroform	chloroform
	Data Collection			
diffractometer	$P2_1$	CAD-4	CAD-4	CAD-4
radiation	Mo Kα(λ = 0.71073 Å), graphite monochromated			
μ, cm^{-1}	0.78	0.81	0.77	0.79
scan mode	$\omega/2\theta$	ω/θ	ω/θ	ω/θ
scan range	2θ from 0.8 below Kα_1 to 0.9 above Kα_2	ω-scan angle = 1.50[1.00 + 0.35tan (θ)]		
scan rate, deg/min	2–15	2–8	3–16	3–16
std rflns, monitored	15 before and after collect	3 (every 1000)	3 (every 500)	3 (every 500)
intensities measd	2658	5029	3112	3731
unique measts	2223	2068	2615	3168
obsd rfletns	1048	1082	1064	1522
R	0.0444	0.0414	0.0382	0.0405
R_w	0.0407	0.0412	0.0356	0.0392
GOF	1.353	1.412	1.271	1.195

ference map at a reasonable bonding distance from N(1) and could be refined satisfactorily with unit occupancy to give an N–H distance of 1.02 (4) Å. For the data collected at 300 K, the initial position on a difference map was further from N(1) and refinement gave an N–H distance of 1.13 (4) Å. In the refinement of **4** at both temperatures, the electron density on a difference map between N and O was more diffuse. Refinement with partial occupancy at two sites was attempted. For the 300 K data this treatment converged at a 3:1 occupancy ratio favoring the oxygen site, while the 193 K data indicated essentially total occupancy at oxygen. These results by themselves indicate that **1** exists mainly as **1a** and **4** exists mainly as **4b** and provide a further indication that the fraction of **1b** in the crystal of **1** may greater at 300 K than at 213 K. However, we consider the information from the bond lengths (discussed in the results section) as more significant in determining the relative proportions of **1a**/**1b** and **4a**/**4b**. In the final refinement, the tautomeric hydrogen was included with full occupancy on N for **1** and on O for **4**. Convergence, indicated by maximum parameter shifts corresponding to 0.05σ, resulted in the final residual values of R, R_w, and GOF quoted on Table I. The weighting schemes used in all refinements had w inversely proportional to $[\sigma(F_o)^2 + 0.0004|F_o|^2]$. In all cases the final difference Fourier map was essentially featureless. The atomic scattering factors for the neutral atoms were those of Cromer and Waber.[42]

Final atomic coordinates for **1** at 213 K and for **4** at 193 K can be found in Tables II and III, respectively. Tables IV and V contain calculated bond lengths and angles. Tables of observed and calculated structure factors, anisotropic thermal parameters for non-hydrogen atoms, and isotropic thermal parameters for hydrogen atoms for **1** at 300 and 213 K and for **4** at 300 and 193 K, as well as atomic coordinates and bond lengths and angles for **1** and **4** at 300 K, have been deposited as supplementary material (see the paragraph at the end of the paper concerning supplementary material).

Results and Discussion

Solution ^{13}C NMR Results. The ^{13}C NMR chemical shifts for **1** at room temperature had already been assigned,[19-24] and the equilibrium constant K of the tautomeric reaction was calculated from the resonances of the phenyl ring carbons.[22] These results were in agreement with estimations based on ^{1}H,[16] ^{14}N,[17] and ^{15}N[22] NMR data. The chemical shifts of the carbon atoms of the naphthalene ring are also known to be sensitive to the position of this equilibrium, particularly that of C(2), which spans a range of ca. 30 ppm from the pure azo to the pure hydrazone form. When strong electron-withdrawing groups are attached to C(4′),

Table II. Fractional Atomic Coordinates for 1-(Phenylazo)-2-naphthol (**1**) at 213 K

	x/a	y/b	z/c
C(1)	0.3530 (1)	0.0625 (5)	0.4100 (2)
C(2)	0.3005 (1)	0.0123 (6)	0.3837 (2)
C(3)	0.2860 (1)	−0.1838 (6)	0.3296 (2)
C(4)	0.3190 (1)	−0.3193 (6)	0.3051 (3)
C(4a)	0.3714 (1)	−0.2774 (5)	0.3313 (2)
C(5)	0.4048 (1)	−0.4254 (6)	0.3074 (3)
C(6)	0.4544 (1)	−0.3840 (6)	0.3310 (3)
C(7)	0.4715 (1)	−0.1894 (6)	0.3787 (2)
C(8)	0.4391 (1)	−0.0407 (6)	0.4033 (3)
C(8a)	0.3883 (1)	−0.0830 (5)	0.3814 (2)
C(1′)	0.3619 (1)	0.5508 (5)	0.5477 (2)
C(2′)	0.4122 (1)	0.5924 (6)	0.5737 (2)
C(3′)	0.4285 (1)	0.7787 (6)	0.6258 (2)
C(4′)	0.3956 (2)	0.9221 (6)	0.6525 (2)
C(5′)	0.3457 (2)	0.8788 (6)	0.6273 (3)
C(6′)	0.3283 (1)	0.6924 (6)	0.5743 (3)
N(1)	0.3422 (1)	0.3676 (5)	0.4927 (2)
N(2)	0.3722 (1)	0.2361 (4)	0.4622 (2)
O	0.2691 (1)	0.1340 (4)	0.4084 (2)
H(3)	0.251 (1)	−0.224 (5)	0.313 (2)
H(4)	0.309 (1)	−0.454 (5)	0.272 (2)
H(5)	0.393 (1)	−0.556 (5)	0.278 (2)
H(6)	0.477 (1)	−0.491 (5)	0.313 (2)
H(7)	0.508 (1)	−0.160 (6)	0.397 (2)
H(8)	0.450 (1)	0.089 (6)	0.432 (3)
H(2′)	0.434 (1)	0.485 (5)	0.552 (2)
H(3′)	0.465 (1)	0.805 (5)	0.643 (2)
H(4′)	0.408 (1)	1.052 (5)	0.692 (2)
H(5′)	0.321 (1)	0.973 (6)	0.643 (2)
H(6′)	0.293 (1)	0.653 (5)	0.558 (2)
HN(1)	0.305 (1)	0.330 (7)	0.478 (3)

(42) Cromer, D. T.; Waber, J. T. *International Tables for X-ray Crystallography*; The Kynoch Press: Birmingham, England, 1974; Vol. IV, Table 2.2 B.

Table III. Fractional Atomic Coordinates for 1-((4′-(Dimethylamino)phenyl)azo)-2-naphthol (**4**) at 193 K

	x/a	y/b	z/c
C(1)	0.1796 (3)	1.0288 (3)	0.3687 (1)
C(2)	0.0117 (3)	1.0597 (3)	0.3826 (1)
C(3)	−0.1176 (4)	1.1493 (4)	0.3459 (1)
C(4)	−0.0786 (4)	1.2092 (4)	0.2973 (1)
C(4a)	0.0886 (3)	1.1804 (3)	0.2805 (1)
C(5)	0.1306 (4)	1.2409 (4)	0.2302 (1)
C(6)	0.2909 (4)	1.2094 (4)	0.2146 (1)
C(7)	0.4192 (4)	1.1171 (4)	0.2498 (1)
C(8)	0.3853 (4)	1.0589 (3)	0.2996 (1)
C(8a)	0.2191 (3)	1.0876 (3)	0.3164 (1)
C(1′)	0.4141 (3)	0.8075 (3)	0.4838 (1)
C(2′)	0.5863 (4)	0.7776 (3)	0.4729 (1)
C(3′)	0.7049 (4)	0.6896 (3)	0.5101 (1)
C(4′)	0.6590 (3)	0.6239 (3)	0.5597 (1)
C(5′)	0.4869 (4)	0.6593 (3)	0.5705 (1)
C(6′)	0.3691 (4)	0.7490 (3)	0.5331 (1)
C(7′)	0.7249 (5)	0.4666 (4)	0.6461 (1)
C(8′)	0.9467 (4)	0.4821 (5)	0.5819 (1)
N(1)	0.2800 (3)	0.8936 (3)	0.4487 (1)
N(2)	0.3169 (3)	0.9419 (3)	0.4020 (1)
N(3)	0.7776 (3)	0.5342 (3)	0.5963 (1)
O	−0.0341 (3)	1.0074 (3)	0.4307 (1)
H(3)	−0.240 (3)	1.166 (3)	0.357 (1)
H(4)	−0.163 (3)	1.267 (3)	0.275 (1)
H(5)	0.039 (3)	1.300 (3)	0.208 (1)
H(6)	0.315 (3)	1.247 (3)	0.179 (1)
H(7)	0.533 (3)	1.090 (3)	0.239 (1)
H(8)	0.473 (3)	0.998 (3)	0.324 (1)
H(2′)	0.617 (3)	0.820 (3)	0.439 (1)
H(3′)	0.820 (3)	0.671 (3)	0.503 (1)
H(5′)	0.449 (3)	0.621 (3)	0.605 (1)
H(6′)	0.255 (3)	0.771 (3)	0.541 (1)
H(7′A)	0.827 (4)	0.420 (4)	0.669 (1)
H(7′B)	0.627 (4)	0.375 (4)	0.638 (1)
H(7′C)	0.676 (3)	0.553 (4)	0.669 (1)
H(8′A)	1.015 (4)	0.428 (4)	0.614 (1)
H(8′B)	0.931 (4)	0.417 (4)	0.547 (1)
H(8′C)	1.023 (4)	0.581 (4)	0.575 (1)
HO	0.071 (5)	0.953 (4)	0.450 (1)

Table IV. Bond Lengths and Bond Angles between Non-Hydrogen Atoms for 1-(Phenylazo)-2-naphthol (**1**) at 213 K

Bond Lengths, Å			
C(1)–C(2)	1.457 (5)	C(2)–C(3)	1.433 (5)
C(3)–C(4)	1.343 (5)	C(4)–C(4a)	1.445 (5)
C(4a)–C(5)	1.394 (5)	C(5)–C(6)	1.368 (5)
C(6)–C(7)	1.394 (5)	C(7)–C(8)	1.380 (5)
C(8)–C(8a)	1.400 (4)	C(1)–C(8a)	1.453 (4)
C(4a)–C(8a)	1.408 (4)	C(1′)–C(2′)	1.387 (5)
C(2′)–C(3′)	1.379 (5)	C(3′)–C(4′)	1.384 (5)
C(4′)–C(5′)	1.379 (6)	C(5′)–C(6′)	1.392 (5)
C(1′)–C(6′)	1.390 (5)	C(1)–N(2)	1.338 (4)
C(1′)–N(1)	1.406 (4)	N(1)–N(2)	1.308 (4)
C(2)–O	1.261 (4)		
Bond Angles, deg			
C(2)–C(1)–C(8a)	120.2 (3)	C(2)–C(1)–N(2)	123.9 (3)
C(8a)–C(1)–N(2)	116.0 (3)	C(1)–C(2)–C(3)	117.1 (3)
C(1)–C(2)–O	121.6 (3)	C(3)–C(2)–O	121.3 (3)
C(2)–C(3)–C(4)	122.2 (3)	C(3)–C(4)–C(4a)	122.3 (3)
C(4)–C(4a)–C(5)	120.9 (3)	C(4)–C(4a)–C(8a)	118.6 (3)
C(5)–C(4a)–C(8a)	120.5 (3)	C(4a)–C(5)–C(6)	120.8 (3)
C(5)–C(6)–C(7)	119.2 (3)	C(6)–C(7)–C(8)	121.0 (3)
C(7)–C(8)–C(8a)	120.5 (3)	C(1)–C(8a)–C(4a)	119.5 (3)
C(1)–C(8a)–C(8)	122.6 (3)	C(4a)–C(8a)–C(8)	117.9 (3)
C(2′)–C(1′)–C(6′)	120.8 (3)	C(2′)–C(1′)–N(1)	122.4 (3)
C(6′)–C(1′)–N(1)	116.8 (3)	C(1′)–C(2′)–C(3′)	118.9 (3)
C(2′)–C(3′)–C(4′)	121.1 (3)	C(3′)–C(4′)–C(5′)	119.8 (3)
C(4′)–C(5′)–C(6′)	120.1 (4)	C(1′)–C(6′)–C(5′)	119.3 (3)
C(1′)–N(1)–N(2)	118.9 (3)	C(1)–N(2)–N(1)	118.4 (3)

the equilibrium, both in solution and in the solid state, is shifted almost completely to the hydrazone structure[15,17] with a C(2) chemical shift of ca. 180 ppm.[21,25,36] On the other hand, the corresponding value for the azo form has been estimated to be approximately 147 ppm.[25] Therefore, we have used the following equation to calculate equilibrium constants for the tautomeric proton exchange reactions:

$$K = [180 - \delta C(2)]/[\delta C(2) - 147] \quad (1)$$

Table V. Bond Lengths and Bond Angles between Non-Hydrogen Atoms for 1-((4′-(Dimethylamino)phenyl)azo)-2-naphthol (**4**) at 193 K

Bond Lengths, Å			
C(1)–C(2)	1.395 (3)	C(2)–C(3)	1.412 (3)
C(3)–C(4)	1.354 (4)	C(4)–C(4a)	1.416 (4)
C(4a)–C(5)	1.403 (4)	C(5)–C(6)	1.358 (4)
C(6)–C(7)	1.399 (4)	C(7)–C(8)	1.362 (4)
C(8)–C(8a)	1.410 (3)	C(8a)–C(4a)	1.420 (3)
C(1)–C(8a)	1.435 (3)	C(1′)–C(2′)	1.397 (3)
C(2′)–C(3′)	1.365 (3)	C(3′)–C(4′)	1.413 (3)
C(4′)–C(5′)	1.405 (3)	C(5′)–C(6′)	1.372 (3)
C(1′)–C(6′)	1.384 (3)	C(1)–N(2)	1.398 (3)
C(1′)–N(1)	1.400 (3)	C(4′)–N(3)	1.363 (3)
C(7′)–N(3)	1.443 (3)	C(8′)–N(3)	1.447 (3)
N(1)–N(2)	1.277 (2)	C(2)–O	1.342 (3)
Bond Angles, deg			
C(8a)–C(1)–C(2)	119.3 (2)	N(2)–C(1)–C(2)	125.0 (2)
N(2)–C(1)–C(8a)	115.6 (2)	C(3)–C(2)–C(1)	120.4 (2)
O–C(2)–C(1)	122.3 (2)	O–C(2)–C(3)	117.3 (2)
C(4)–C(3)–C(2)	120.3 (3)	C(4a)–C(4)–C(3)	122.0 (3)
C(4a)–C(5)–C(6)	121.5 (3)	C(7)–C(6)–C(5)	119.6 (3)
C(8)–C(7)–C(6)	120.8 (3)	C(8a)–C(8)–C(7)	120.8 (3)
C(8)–C(8a)–C(1)	122.2 (2)	C(4a)–C(8a)–C(1)	119.5 (2)
C(4a)–C(8a)–C(8)	118.3 (2)	C(5)–C(4a)–C(4)	122.6 (3)
C(8a)–C(4a)–C(4)	118.5 (2)	C(8a)–C(4a)–C(5)	118.9 (3)
C(6′)–C(1′)–C(2′)	118.5 (2)	N(1)–C(1′)–C(2′)	125.5 (2)
N(1)–C(1′)–C(6′)	115.9 (2)	C(3′)–C(2′)–C(1′)	120.1 (3)
C(4′)–C(3′)–C(2′)	122.1 (3)	C(5′)–C(4′)–C(3′)	116.9 (2)
N(3)–C(4′)–C(3′)	121.6 (3)	N(3)–C(4′)–C(5′)	121.4 (2)
C(6′)–C(5′)–C(4′)	120.5 (2)	C(5′)–C(6′)–C(1′)	121.8 (3)
N(2)–N(1)–C(1′)	116.6 (2)	N(1)–N(2)–C(1)	114.5 (2)
C(7′)–N(3)–C(4′)	120.1 (2)	C(8′)–N(3)–C(4′)	120.8 (2)
C(8′)–N(3)–C(7′)	118.4 (2)		

Table VI. ^{13}C CP MAS (50.2 MHz) and ^{13}C Solution Chemical Shift Assignments (δ)

	compound				
	2	**3**	**3**[a]	**4**	**4**[a]
1	128.8	128.9	129.44	128.6	129.35
2	163.5	161.4	160.97	154.7	156.12
3	121.6	121.9	121.57[b]	121.6	120.97[d]
4	139.5	137.7	136.47	131.3	133.95
4a	128.8	128.9	*f*	128.6	*g*
5	128.8	128.9	128.04[c]	128.6	127.42[e]
6	128.8	126.9	124.69	123.1	124.12
7	128.8	128.9	128.24[c]	128.6	128.05[e]
8	124.1	124.1	122.05[b]	123.1	121.72[d]
8a	134.3	134.2	133.02	132.8	133.26
1′	139.5	139.1	141.71	139.8	139.65
2′, 6′[h]	116.8	117.2	122.05	116.8	123.08
	128.8	128.9		128.6	
3′, 5′	108.4; 109.9[i]	109.8	115.20	109.9	112.02
	120.3	119.8		112.6	
4′	161.2	161.4	160.07	151.7; 149.3[i]	151.62
Me_2N				38.4; 40.3[j]	40.24
CH_2		64.8	63.84		
CH_3	55.5	15.5	14.73		

[a] CD_2Cl_2 solution at room temperature measured at 75.5 MHz. [b–e] Assignments within one column may be interchanged. [f] Not observed but probably overlapped with the signal at 128.04 ppm. At −50 °C a quaternary carbon signal can be clearly distinguished at 127.67 ppm, corresponding to C(4a). [g] Not observed but overlapped with the peak at 128.04 ppm. As in *b*, this signal appears at 127.61 ppm at −50 °C. [h] The signals appearing at ca. 117 ppm are clearly seen in the spectra; those at ca. 129 ppm are assumed to be overlapped with the intense peak at this frequency (see text). [i] The doubling of this signal is attributed to the existence of incongruent molecules in the asymmetric unit. [j] These splittings are due to the effect of the coupling to the ^{14}N bonded to these carbons.

Table VII. Solution ^{13}C NMR Chemical Shifts of C(2) in **1** at Different Temperatures and Equilibrium Constants Calculated with Eq 1

T, K	δ C(2), ppm	K	T, K	δ C(2), ppm	K
303	170.80	0.39	223	173.52	0.24
293	170.99	0.38	203	174.37	0.21
263	171.96	0.32	183	175.34	0.16
243	172.69	0.28			

The value of $K = 0.38$ so obtained for **1** at room temperature in CD_2Cl_2 [$\delta C(2) = 170.99$ ppm] is in agreement with previous determinations.[16,17,19-24]

^{13}C NMR data have also been reported for **2** in $CDCl_3$ solution at room temperature.[21] As compounds **3** and **4** have not been previously analyzed, we report the ^{13}C chemical shift assignments in Table VI, based on a comparison with literature data on related structures and especially on a recent rigorous study of **1**.[24]

Variable-temperature ^{13}C NMR spectra were recorded at 75.5 MHz for **1–4**. The chemical shifts of C(2) and the equilibrium constants for **1** in CD_2Cl_2 solution computed by using eq 1 are presented in Table VII. A consistent downfield shift of the C(2) resonance suggesting a displacement of the equilibrium toward the hydrazone **1a** is observed with decreasing temperature. Values of K shown in Table VII give $\Delta H° = 0.82 \pm 0.02$ kcal mol^{-1} and $\Delta S° = 0.80 \pm 0.08$ eu for the reaction. This value of $\Delta H°$ is in agreement with that previously obtained (0.69 kcal mol^{-1}) on the basis of the change in $J(^1H,^{15}N)$ between the labile proton and $^{15}N(1)$ with temperature.[16] Thermodynamic data for this process have also been reported in $CDCl_3$ solution by monitoring the change in $^{15}N(1)$ and $^{15}N(2)$ chemical shifts with temperature.[20,37] Although some discrepancies may arise due to the selection of temperature-independent chemical shifts for structures **1a** and **1b** in eq 1, the results agree in showing that the fraction of **1a** increases as the temperature decreases.

In the case of compounds **2**, **3**, and **4**, the chemical shifts of C(2) showed small changes with temperature, indicating that the equilibrium mixtures have approximately constant compositions; at 293 K δ C(2) is 161.16 in **2** ($K = 1.33$), 161.10 in **3** ($K = 1.34$), and 156.06 in **4** ($K = 2.65$). However, caution must be used in interpreting such results since chemical shifts may be affected by a dependence on temperature beyond that resulting from a shift of the equilibrium being studied. In any case it is interesting that there is a slight preference for the azo structures in these compounds.

The solution study shows, therefore, that the single-proton-transfer process is fast on the NMR time scale in **1–4**, over the temperature range studied, as revealed by the presence of only one sharp resonance assigned to C(2). Furthermore, the relative amounts of azo and hydrazone forms present at equilibrium, measured by the chemical shift of C(2), depend on the nature of the substituent attached to C(4′). Thus, interest was focused on the comparison of this behavior with that in the solid state.

Solid-State ^{13}C NMR Measurements. The high-resolution ^{13}C CP MAS NMR spectrum of **1** at 50.2 MHz is shown in Figure 1a. To facilitate the chemical shift assignments, the dipolar-dephased spectrum was also recorded (Figure 1b). In this latter case only quaternary carbons (and, if present, methyl groups) appear in the spectrum, since signals due to CH and CH_2 carbons decay during a short delay (ca. 40 μs) during which no high power proton decoupling is applied.[43] Signals from quaternary carbons are observed at 174.1, 143.0, 134.2, and 128.2 ppm (Figure 1b) and are attributed, respectively, to carbons C(2), C(1′), and C(8a) and the overlapping resonances of C(1) and C(4a), by comparison with solution data. The presence of a sharp signal assigned to C(2) with a chemical shift comparable to that observed in CD_2Cl_2 solution at −70 °C implies that **1** also undergoes a fast proton exchange in the solid phase.

The analysis of the protonated carbon resonances is complicated, however, by an extensive superposition of signals in the region

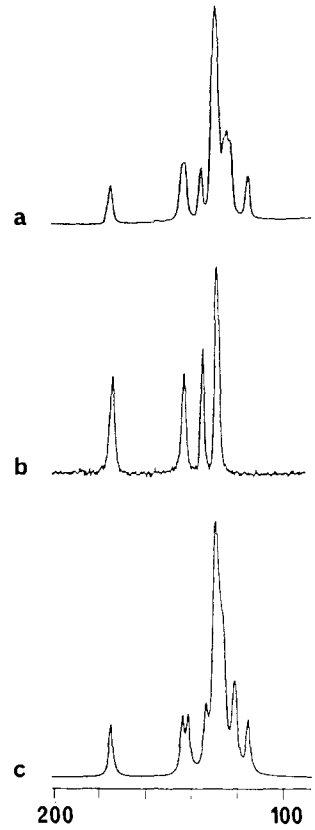

Figure 1. (a) High-resolution solid-state ^{13}C NMR spectrum of 1-(phenylazo)-2-naphthol (**1**) at 50.2 MHz. (b) Dipolar-dephased spectrum of **1** obtained inserting a delay of ca. 40 μs prior to the acquisition (only quaternary carbons appear). (c) Simulated spectrum obtained by convoluting the CD_2Cl_2 solution ^{13}C spectrum at −70 °C with a line width of 80 Hz. All carbons were given the same relative intensity, while a splitting of ±3 ppm was introduced in the signal corresponding to the pair C(2′),C(6′).

114–129 ppm. To compare solution and solid-state NMR data, a simulation was performed by selecting the solution chemical shifts at the temperature that gives the best fit to the solid-state spectrum (after application of a suitable line broadening). Figure 1c shows the simulated spectrum using the values measured at −70 °C in CD_2Cl_2. It was necessary to include a splitting of ±3 ppm in the resonances of the pair C(2′),C(6′) which in solution are rotationally equivalent. This latter effect is known to occur in crystals of aromatic substituted compounds and is due to the lack of the rotational freedom present in solution.[44]

A noteworthy feature of the ^{13}C NMR spectrum shown in Figure 1b is the lack of splittings in the carbons bonded to ^{14}N,C(1), and C(1′). In ^{14}N-containing samples, asymmetric splittings or non-Lorentzian broadening effects are often observed in the ^{13}C signals, due to a residual dipolar coupling between ^{13}C and adjacent ^{14}N nuclei which cannot be completely averaged out by the MAS experiment.[45-47] Theoretical values for the expected partition can be calculated provided that information is available regarding quadrupole parameters for the ^{14}N nuclei, the ^{13}C–^{14}N distance, and the relative orientation of the vector joining both nuclei in the principal axis system (PAS) of the ^{14}N quadrupole tensor. It has been shown that the value of the splitting S can be given by the following equation:[47]

$$S = (9D\chi/20Z)(3\cos^2\beta^D - 1 + \eta\sin^2\beta^D\cos 2\alpha^D) \quad (2)$$

(43) Opella, S. J.; Frey, M. H. *J. Am. Chem. Soc.* **1979**, *101*, 5854.

(44) Hays, G. R. *J. Chem. Soc., Perkin Trans. 2* **1983**, 1049.

(45) Opella, S. J.; Frey, M. H.; Cross, T. A. *J. Am. Chem. Soc.* **1979**, *101*, 5856.

(46) Groombridge, C. J.; Harris, R. K.; Packer, K. J.; Say, B. J.; Turner, S. F. *J. Chem. Soc., Chem. Commun.* **1980**, 174.

(47) Olivieri, A. C.; Frydman, L.; Diaz, L. E. *J. Magn. Reson.* **1987**, *75*, 50.

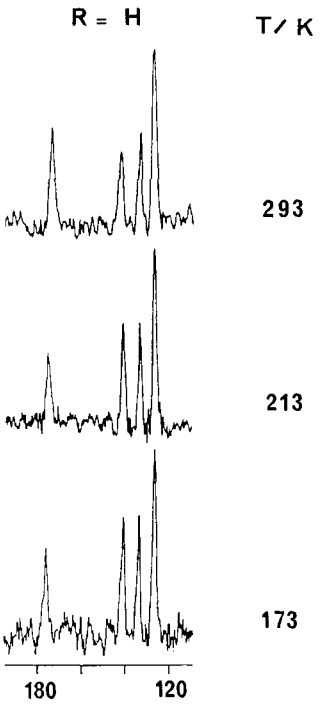

Figure 2. ^{13}C CP MAS NMR spectra (75.5 MHz) of **1** at the temperatures indicated. Spectra were run in the dipolar-dephasing mode, allowing a short delay with no proton decoupling (only quaternary carbons appear).

where D is the dipolar $^{13}C,^{14}N$ coupling constant, χ is the ^{14}N quadrupole coupling constant, Z is the Zeeman ^{14}N frequency in the applied field, η is the asymmetry parameter of the quadrupole interaction, and β^D and α^D define the orientation of the C–N vector in the PAS. The analysis of eq 2 shows that splittings corresponding to =N— groups are too small to be detected.[48] Therefore, only C(1′) in the hydrazone form **1a** may be expected to show the effect. There are, however, two alternative explanations for the lack of partition at C(1′). If the ^{14}N spin–lattice relaxation time is sufficiently long, then in the fast-exchange limit the splittings will be averaged according to the populations of both tautomeric forms. This will lead to an effective splitting $S_{eff} = p_h S_h + p_a S_a$ at C(1′), where S_h and S_a are the splittings induced by N(1) in the hydrazone form (with population p_h) and azo form (with population p_a). Since S_a is expected to be small, the effective splitting may be obscured by the natural line width of the ^{13}C signal. On the other hand, there is the interesting possibility that the proton-transfer reaction taking place in the solid provides a relaxation mechanism for the ^{14}N nuclei, causing a "self-decoupling" of the ^{13}C line. As suggested, this phenomenon is likely to occur in chemically exchanging systems[49] and would result in a collapse of the split resonance into a sharp one at the isotropic frequency.[50]

Since the comparison of solution and solid-state NMR data leads to the conclusion that a rapid tautomeric proton-exchange reaction is present in the solid as well as in solution, a variable-temperature ^{13}C CP MAS NMR study was performed to obtain information about the energetics of the process. Figure 2 shows dipolar-dephased spectra recorded at 75.5 MHz at three different temperatures. The observed chemical shifts for C(2) exhibit, as in solution, a downfield trend with decreasing temperatures [δ C(2) is 174.1 at 293 K (K = 0.22), 176.2 at 213 K (K = 0.13), and 177.8 at 173 K (K = 0.07)], suggesting an increase in the population of the hydrazone form **1a** on lowering the temperature. The analysis of these data indicates an approximate value of $\Delta H°$ of 0.9 kcal mol^{-1}, comparable to the solution result, and in agreement with that found by ^{15}N CP MAS spectroscopy.[37] The observed tautomeric composition shows a small increase in the fraction of the hydrazone structure **1b** in going from solution to the solid state, again in agreement with previous results.[37]

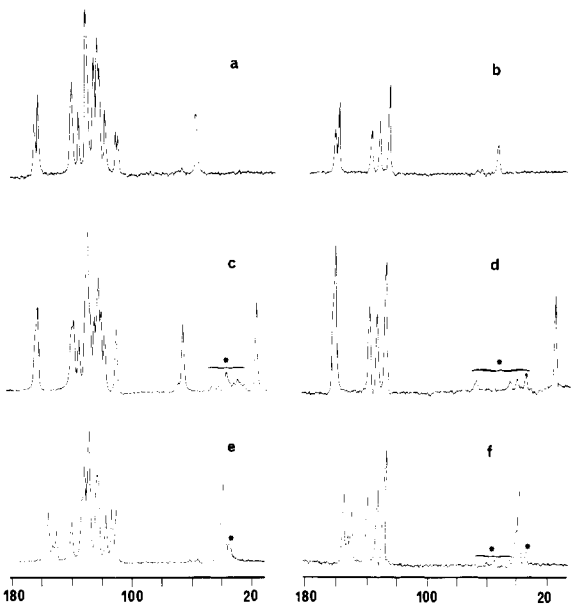

Figure 3. High-resolution solid-state ^{13}C NMR spectra of compounds **2–4** at 50.2 MHz. (a, c, e) spectra obtained in the conventional CP MAS mode for **2**, **3**, and **4**, respectively; (b, d, f) corresponding dipolar-dephased spectra (methyl groups and quaternary carbons appear). Peaks marked with asterisks are spinning sidebands.

As regards compounds **2–4**, 50.2-MHz ^{13}C CP MAS spectra and dipolar-dephased data are presented in Figure 3. Quaternary carbons as well as methyl groups are easily located from the spectra shown in Figure 3b,d,f. The resonances attributed to C(2) appear as sharp singlets close to their solution values, indicating again that all of these compounds undergo a rapid proton transfer on the NMR time scale in the solid state. Equilibrium constants calculated from the C(2) chemical shifts are as follows: **2**, K = 0.98 (163.5 ppm); **3**, K = 1.21 (161.4 ppm); **4**, K = 3.12 (154.7 ppm). If the small differences between the C(2) chemical shifts in both phases are due to different equilibrium compositions, then the values suggest a small increase in the fraction of hydrazone in **2** and **3** and in the fraction of azo molecules in **4**. As with **1**, the carbons bonded to nitrogens N(1) and N(2) do not exhibit any splitting or unusual broadening. However, carbons bonded to N(3) in **4** appear split by the residual dipolar mechanism described above, e.g., C(4′) at 150.1 ppm and Me_2N at 39.0 ppm (Figure 3f). Equation 2 could be used to account for these splittings if corresponding data for the ^{14}N quadrupole tensor were known. Quadrupole coupling constants for *N,N*-dimethylamino groups in aromatic compounds having the general structure 4-R(C_6H_4)NMe_2 have been reported as ranging from 4.4 MHz (R = NO_2) to 5.4 MHz (R = OMe).[51] Since **4** may be considered to consist largely of molecules of 4-R′—N=N—(C_6H_4)NMe_2, the value of χ is expected to be close to 4.4 MHz. Asymmetry factors were found to be very small (0.01–0.04),[51] in agreement with the symmetric environment around N(3) in the molecular plane. The angle β^D may be set at 90°, as the most likely orientation of the z axis of the quadrupole tensor is along the lone pair of electrons. Finally, C–N distances are taken from the X-ray structure for this compound (vide infra). Introduction in eq 2 of the values Z = 14.5 MHz, χ = −4.3 MHz, η = 0, β^D = 90° leads to the following calculated splittings: C(4′), + 113 Hz [r(C–N) = 1.371 Å] and Me_2N, +96 Hz [r(C–N) = 1.446 Å (average of both C–N bond distances)]. The observed values are

(48) Olivieri, A. C.; Frydman, L.; Grasselli, M.; Diaz, L. E. *Magn. Reson. Chem.* **1988**, *26*, 281.
(49) Jonsen, P. *J. Magn. Reson.* **1988**, *77*, 348.
(50) Olivieri, A. C. *J. Magn. Reson.*, in press.
(51) Osokin, D. Ya.; Safin, I. A.; Tintinskii, V. B.; Gavrilov, V. I.; Galyametdinov, Yu. G.; Chernokal'skii, B. D. *Izv. Akad. Nauk. SSSR, Ser. Fiz.* **1975**, *39*, 2565.

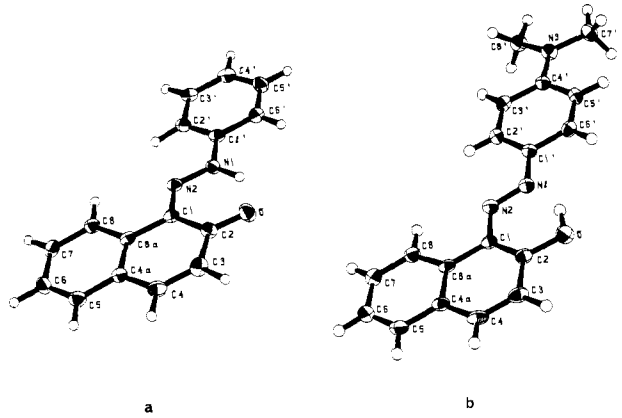

a b

Figure 4. ORTEP plots of single molecules of (a) **1** at 213 K and (b) **4** at 193 K. The labile hydrogen is shown as bonded to N(1) in **1** and to O in **4**, according to difference Fourier results.

+110 and +95 Hz, respectively, showing the excellent agreement previously noticed in the study of other ^{14}N-containing solid materials.[48]

The comparison of CP MAS and dipolar-dephased spectra allows the resonances due to CH and CH_2 groups to be assigned. The assignments are shown in Table VI and are mainly based on a comparison with solution results. The following interesting differences between solution and solid-state chemical shifts are noted, however: the resonances due to the pair C(2′),C(6′) appear invariably split into two signals, one at ca. 117 ppm whereas the other one is probably buried in the intense signal at ca. 129 ppm. The average of these two values (123 ppm) is close to the rotationally averaged solution value (122–123 ppm, Table VI). Another splitting of ca. 10 ppm is observed in the signals of C(3′),C(5′) in **2** and **3** as expected from previous observations in alkoxy-substituted aromatic compounds.[44] A correspondingly smaller partition is measured for these carbons in **4**, since the Me_2N group should affect C(3′) and C(5′) to almost the same extent.

As with **1**, variable-temperature studies were carried out on the dipolar-dephased spectra of **2**–**4**. No appreciable changes were noticed in the resonances of either **2** or **3**, whereas in the case of **4** a weak variation was detected in the C(2) resonance, from 155.0 ppm at 293 K to 153.8 ppm at 193 K. These results indicate that the energy difference between tautomers is, as in solution, very small.

X-ray Diffraction Results. To complement the information gathered from the NMR data in the solid state, X-ray crystal structure determinations were carried out for **1** at 213 and 300 K and for **4** at 193 and 300 K.

ORTEP[52] plots of single molecules of **1** at 213 K and of **4** at 193 K are shown in Figure 4, parts a and b, respectively. Tables II and III give fractional atomic coordinates for these two compounds at these temperatures, and Tables IV and V show the corresponding bond lengths and angles. As the bond lengths for **1** and for **4** show very small differences over the respective temperature ranges studied, most of the following discussion refers to the dimensions at the lower temperature. Bond lengths of N(2)–C(1), N(1)–N(2), and C(2)–O might be expected to furnish information regarding the position of the equilibrium between the azo and hydrazone forms **1a** and **1b** in the crystal, since these two structures have formally different bond orders. Since the proton-transfer reaction has been shown by the NMR results described above to be rapid on the X-ray time scale, the average bond lengths should be a weighted average of those of the two molecular structures in equilibrium. It should be noted that bond lengths involving sp^2-hybridized N and C atoms in complex conjugated systems of this type might be modified by the contribution of dipolar resonance structures to each of the two hybrid molecular species.[53]

(52) Johnson, C. K. ORTEP II. A Fortran Thermal Ellipsoid Plot Program for Crystal Structure Illustrations (Report ORNL-5138), Oak Ridge National Laboratory, Oak Ridge, 1976.

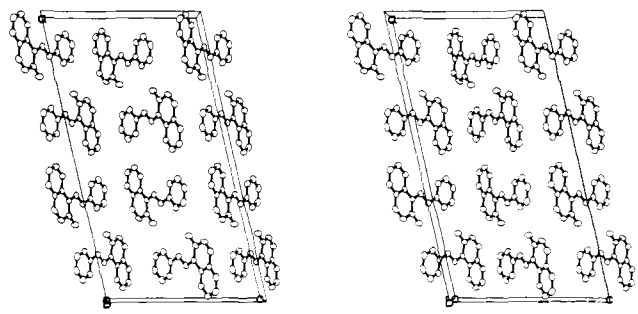

Figure 5. Stereoview of the packing arrangement of **1**. No significant intermolecular interactions are observed.

Thus the effect of a contribution of the resonance form **1a′** to a hybrid **1a** would be to lead to changes in apparent bond lengths in the same direction as a rapid equilibrium with **1b**. To minimize the effects of such resonance on our estimation of the equilibrium constants, comparison was made of these bond lengths with those of azo dyes chosen as model compounds that had conjugated systems somewhat similar to that of **1a**. In the case of **1**, although the equilibrium lies toward the hydrazone **1a**, it can be seen that both C(2)–O and N(2)–C(1) bonds [1.261 (4) and 1.338 (4) Å] are longer, whereas N(1)–N(2) [1.308 (4) Å] is shorter than was found in the model compounds. For example, C(2)–O, N(2)–C(1) and N(1)–N(2) bond lengths are 1.228 (7), 1.309 (5), and 1.318 (6) Å in **5**,[31] 1.23 (1), 1.33 (1), and 1.31 (1) Å in **6**,[29] and 1.26 (1), 1.33 (1), and 1.35 (1) Å in **7**,[33] respectively. A small fraction of **1b** in equilibrium with **1a** at each molecular site would lead to an observed shortening of the N(1)–N(2) bond and a lengthening of C(2)–O and N(2)–C(1), as observed.

As regards the location of the labile proton in **1**, evidence from difference maps and refinement procedures shows it to be bonded predominantly to N(1). (However, the X-ray method is not sensitive enough to detect the electron density that would result from a small percentage of tautomer **1b** with the hydrogen bonded to oxygen.) At 213 K, the position of the proton and the distances N(1)···O [2.551 (4) Å] and HN(1)···O [1.73 (4) Å] suggest an intramolecular hydrogen bond. The X-ray results are thus consistent with those from NMR and with a structure in which at each molecular site in the crystal there occurs a rapid intramolecular N–O proton exchange equilibrium between **1a** and **1b**, with the hydrazone **1a** predominating.

In the crystals of both **1** and **4** there is intramolecular hydrogen bonding between the nitrogen and oxygen atoms directly involved in the tautomeric proton exchange. Inspection of the packing diagrams for both compounds (Figures 5 and 6) reveals no adjacent atom sufficiently close to participate in a more complex *inter*molecular proton transfer. It is therefore concluded that the process is *intra*molecular. The possibility was examined that the positions of the equilibria in **1** and **4** might be influenced by the crystalline environment, but no evidence for significant influences was found. An elegant analysis of the effect of crystal environment on the proton-exchange equilibrium in crystals of dimers of certain carboxylic acids has been discussed by Leiserowitz.[54]

In the case of **4**, the bond lengths indicate that its constituent molecules exist principally in the azo form. However, N(1)–N(2) [1.277 (2) Å] and N(2)–C(1) [1.398 (3) Å] appear to be longer and shorter, respectively, than similar bonds in aromatic azo structures. Reported N=N double bonds fall in the range 1.23–1.24 Å, whereas N–C(sp^2) single bonds lie within the range 1.41–1.46 Å.[55] (A contribution of a resonance structure such as **4b′** might also have some effect on the bond lengths.) The discussion presented above in connection with **1** is also pertinent here. A rapid equilibration at each crystal site between molecules

(53) Burke-Laing, M.; Laing, M. *Acta Crystallogr.* **1976**, *B32*, 3216.
(54) Leiserowitz, L. *Acta Crystallogr.* **1976**, *B32*, 775–801.
(55) Graeber, E. J.; Morosin, B. *Acta Crystallogr.* **1974**, *B30*, 310. Gilardi, R. D.; Karle, I. L. *Ibid.* **1972**, *B28*, 1635. Schilling, J. W.; Nordman, C. E. *Ibid.* **1972**, *B28*, 2177. Hanson, A. W. *Ibid.* **1973**, *B29*, 454.

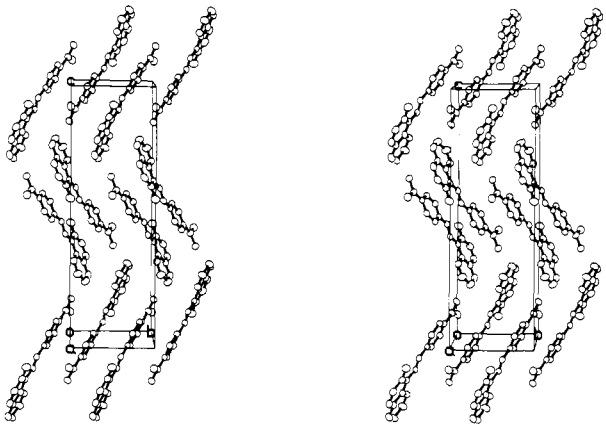

Figure 6. Stereoview of the packing arrangement of **4**. As with **1**, no relevant interactions are detected.

4a and **4b**, the major component being the azo form, is consistent with both the X-ray and the NMR results discussed above.

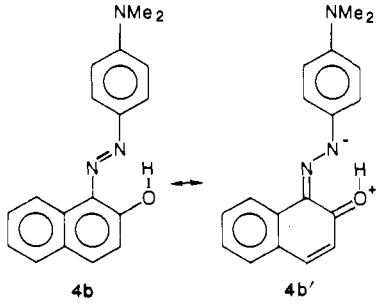

The difference maps and refinement procedures for **4** indicated that the labile hydrogen was bonded principally to oxygen, with N(1)···O and HO···N(1) distances at 193 K of 2.525 (3) and 1.66 (3) Å, respectively. As with **1**, no significant interactions that might be expected to affect seriously the equilibrium between **4a** and **4b** were detected on examination of the crystal packing (Figure 6).

While the molecular dimensions of **4** show no significant differences over the temperature range studied, those for **1**, particularly the C(2)–O bond (1.284 (4) Å at 300 K and 1.261 (4) Å at 213 K), do show some small differences. While most of these differences are not individually statistically significant, the trends are all in the direction that favors a higher proportion of **1a** at the lower temperature. In addition, as described in the experimental section, there was some evidence from the refinement procedures to suggest that the labile hydrogen was more closely associated with N(1) at 213 K than at 300 K, probably indicating a higher proportion of **1a** at the lower temperature. Thus all the crystallographic evidence is consistent with the conclusions from the variable temperature ^{13}C CP MAS results indicating a somewhat higher proportion of **1a** in the solid at 213 K. In as much as the peripheral C=O bond is shorter at the lower temperature, it is unlikely that the difference in length is due to the effects of thermal motion. (For a general discussion of thermal motion in crystals see ref 56.)

Conclusion. The combined use of NMR and X-ray diffraction techniques to study solid-state reactions is of particular value because of their complementary nature. Comparison of solution ^{13}C NMR chemical shifts at varying temperatures with the corresponding CP MAS analysis provides strong evidence that rapid proton switching equilibrates hydrazones **1a–4a** and azo compounds **1b–4b** in the solid state. A minimum value for the exchange rate constant, based on the order of the frequency difference of C(2) from the extreme azo form to its hydrazone counterpart, is approximately 2×10^3 s^{-1}. The equilibrium composition is similar to that measured in solution. Differences in position and/or multiplicity of ^{13}C lines in going from solution to the solid phase can be satisfactorily explained on the basis of loss of rotational freedom, or $^{13}C,^{14}N$ residual dipolar coupling effects.

Crystal structures of the unsubstituted compound **1** and the corresponding 4′-*N*,*N*-dimethylamino derivative **4**, determined by X-ray diffraction, are consistent with the NMR results and provide evidence that the proton transfers are intramolecular and not intermolecular in the crystal. Further there are no intermolecular interactions in the crystal which would be expected to affect significantly the hydrazone–azophenol equilibrium.

Note Added in Proof. We have just become aware of a report (Salmén, R.; Malterud, K. E.; Pedersen, B. F. *Acta Chem. Scand. Ser. A* **1988**, *42*, 493–499) describing the crystal structure of 1-(phenylazo)-2-naphthol (**1**) at 138 K. The X-ray results reported there are fully consistent with those described in the present article.

Acknowledgment. This material is based on research activity supported by the National Science Foundation under Grant CHE-85-10600. A.C.O. is grateful to the Consejo Nacional de Investigaciones Cientificas y Tecnicas (CONICET, Argentina) for a partial fellowship. We thank Patricia Saindo and Dr. Steven Byrn of the Department of Medicinal Chemistry and Pharmacognosy of Purdue University for assistance in obtaining the 50.2-MHz spectra.

Supplementary Material Available: Tables of anisotropic thermal parameters for non-hydrogen atoms, isotropic thermal parameters for hydrogen atoms for **1** at 300 and 213 K and for **4** at 300 and 193 K, as well as atomic coordinates and bond lengths and angles for **1** and **4** at 300 K (10 pages); listing of observed and calculated structure factors (22 pages). Ordering information is given on any current masthead page.

(56) Dunitz, J. D.; Maverick, E. F.; Trueblood, K. N. *Angew. Chem., Int. Ed. Engl.* **1988**, *27*, 880–895.